A&A 392, 1047–1052 (2002)
DOI: 10.1051/0004-6361:20021072

Astronomy & Astrophysics

Research Note

Towards the identification of circumstellar hibonite

H. Mutschke[1], Th. Posch[2], D. Fabian[1], and J. Dorschner[1]

[1] Astrophysikalisches Institut und Universitäts-Sternwarte, Schillergässchen 2-3, 07745 Jena, Germany
[2] Institut für Astronomie, Türkenschanzstraße 17, 1180 Wien, Austria

Received 15 February 2002 / Accepted 20 June 2002

Abstract. We have performed IR reflectance measurements on crystalline $CaAl_{12}O_{19}$ (hibonite) and derived optical constants for both principal directions of the electric field vector relative to the crystallographic *c*-axis. Based on the resulting dielectric functions, we calculated small particle spectra and found six maxima of the absorption cross section for spherical dust grains at the wavelengths 12.3, 15.9, 21.1, 25.1, 34.4, and 78.7 μm. For nonspherical particles, strong shifting and broadening of the two strongest resonances at 12.3 and 15.9 μm occurs. The signal-to-noise-ratio of ISO spectra of oxygen-rich AGB stars is not sufficient for a definite identification of these bands, even though there is some weak indication of their presence. We propose additional observations to clarify this point.

Key words. stars: circumstellar matter – stars: formation – stars: AGB and post-AGB – solar system: formation – methods: laboratory

1. Introduction

Hibonite ($CaAl_{12}O_{19}$) is a refractory oxide which was discovered as a terrestrial mineral as late as 1956, but was identified as a rather important component of meteorites already 15 years later.

In Ca-Al-rich inclusions (CAIs) from carbonaceous chondrites, hibonite is quite common and occurs frequently together with perovskite ($CaTiO_3$), spinel ($MgAl_2O_4$) and other refractory oxides and silicates (Brearley & Jones 1998). Therefore, it belongs to those solids which are expected to be the first ones formed in our solar system. Above 2×10^{-3} bar, hibonite is actually the very first condensate (at $T > 1770$ K) from a cooling solar composition gas. At lower pressures, hibonite is expected to form by reaction of corundum (Al_2O_3) with gas-phase calcium (Fegley 1992). This sequence of formation is reflected by the textures of some hibonite-bearing CAIs, which show corundum inclusions and the presence of the Ca-rich mineral grossite ($CaAl_4O_7$) in outer regions (Krot et al. 2001). The details of the formation of these hibonite-bearing meteoritic inclusions are, however, still a matter of debate (see Fahey et al. 1994; Kurat 1983 and references therein). Apart from hibonite and grossite, two other calcium oxides – $CaAl_2O_4$ and $CaAl_{24}O_{37}$ – have also been identified in meteorites (Ulyanov 1998).

Send offprint requests to: H. Mutschke,
e-mail: mutschke@astro.uni-jena.de

Quite recently, two out of 57 hibonite grains isolated from a primitive meteorite (Semarkona, ordinary chondrite) have been shown to be of presolar origin. Analysis of isotope ratios in these grains proved them to have formed in oxygen-rich AGB star atmospheres (Choi et al. 1999). Consequently, Ca-Al oxides are able to form also in stellar outflows, despite of the much lower gas densities compared to the solar nebula. The apparent rareness of detection of presolar hibonite grains has been explained by these authors by the large background of solar system hibonite in the meteorite. They also expect other circumstellar calcium-bearing minerals to be present but to be destroyed by the isolation process.

The identification of these circumstellar condensates by astronomical observations has to rely on their infrared emission bands corresponding to lattice vibrational transitions. During the past years, it has become clear from the analysis of ISO-SWS spectra that oxygen-rich AGB stars with low mass-loss rates do not only show the well known 10 and 18 μm silicate emission features, but also some other (comparatively weak) bands. In this context, the 13 μm feature deserves special interest. This feature is observed especially in the spectra of SRb variables (see Sloan et al. 1996) and seems to occur only within a limited range of photospheric as well as dust shell temperatures (Hron et al. 1997).

Even if there are alternative proposals for the identification of the 13 μm band (Speck et al. 2000), there is some evidence

for its relation to a dust species dominated by aluminium oxides (e.g. Begemann et al. 1997). In two previous papers (Posch et al. 1999; Fabian et al. 2001a), we have derived average residual emission profiles of oxygen-rich circumstellar dust in the 11–18 μm wavelength region on the basis of ISO spectra. By means of this procedure, we detected one additional dust emission band centered at a position of 16.8 μm which, together with the 13 μm band and another feature at 32 μm, we attributed to spinel ($MgAl_2O_4$). This raises the question which other solid state features attributable to oxides can be identified in stardust spectra.

The goal of this paper is to extend the basis of laboratory data for the purpose of the identification of IR bands and to discuss the possibilities for an identification using recent and future infrared observations.

2. Determination of the optical constants

The crystallographic structure of hibonite is very similar to that of beta-alumina (β-Al_2O_3), which has been described by Bragg et al. (1931) and Beevers & Ross (1937). Among the 64 atoms contained in the elementary cell, 50 are contained in a spinel type lattice. The transition from one "spinel bloc" to the next involves two Ca ions, six Al ions and six oxygen ions. The resulting crystal structure is of hexagonal symmetry. The optical properties along and normal to the c-axis, therefore, are different.

In natural hibonites, Al ions are often partially substituted by Ti and Fe ions. According to Curien et al. (1956), the Ti and Fe^{2+} ions replace Al ions situated at octahedral lattice sites, whereas Fe^{3+} ions can be octahedrally as well as tetrahedrally coordinated.

We studied the infrared optical properties of natural hibonite crystals from Evisa and Antsirabé, Madagascar, with average compositions of $Ca_{0.84}Al_{10.84}Ti_{0.69}Fe_{0.34}O_{19}$ and $Ca_{0.85}Al_{11.37}Ti_{0.26}Fe_{0.38}O_{19}$, respectively. Hibonite Evisa consisted of plates with the large surfaces normal to the c-axis. These unpolished surfaces have been used for reflectance measurements at near-normal incidence with unpolarized light. A gold mirror has been used as the reference. The homogeneity and composition of the crystal has been studied by scanning electron microscopy (SEM) and energy-dispersive X-ray (EDX) analysis, revealing excellent quality of the sample with very little inclusions and the above elemental composition.

Sample Antsirabé has been cut along the c-axis to produce a surface containing this axis. Analysis by SEM and EDX, respectively, revealed some degree of porosity of the crystal and minor impurities of Mg, Si, and Zn. After polishing this surface, reflectance measurements have been performed with IR radiation polarized perpendicular and normal to the c-axis. Comparing the spectrum obtained with the polarization normal to the c-axis ($E\perp c$) to the one of sample Evisa, we found a difference in the absolute values which can be explained by the porosity of the crystal. Multiplying the original reflectance with a factor of 1.3 produced a good agreement of the spectrum with the one of sample Evisa. All the bands seen in sample Evisa are seen in sample Antsirabé and vice versa (see Fig. 1). Because of the better signal-to-noise ratio, we will use the spectra obtained with sample Evisa for the following analysis. The reflectivity of sample Antsirabé at polarization parallel to the c-axis ($E\|c$), consequently, has also been multiplied with a factor of 1.3.

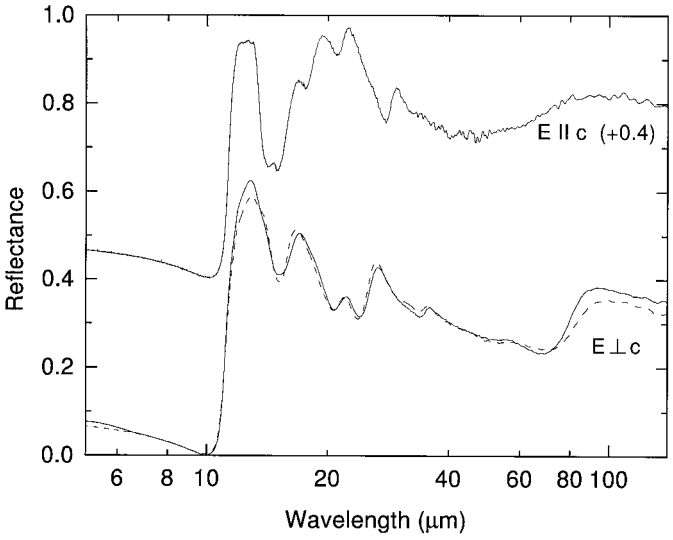

Fig. 1. Infrared reflectance spectra of hibonite single crystals at near-normal incidence for polarization parallel and perpendicular to the c-axis, respectively. The spectra originate from measurements at samples Evisa (solid curve labeled $E\perp c$) and Antsirabé (dashed curve $E\perp c$ and solid curve $E\|c$). The latter two have been multiplied by a factor of 1.3 to account for the lower quality of the sample surface.

The $E\perp c$ spectrum shows some similarities with the spectra of defect (Mg-poor) spinels discussed by Fabian et al. (2001a). The two maxima situated at wavelengths smaller than 20 μm obviously correspond to the Al–O vibrations seen in these spectra. This is not surprising, since Mg-free spinel "blocs" form the basic units of the hibonite lattice, as was mentioned in Sect. 1. As also expected for such defect spinels, the feature is positioned at shorter wavelengths than those of normal spinels because of the occupation of tetrahedral interstices in the cubic closed-packed oxygen lattice (this corresponds to the dominance of the "G" mode over the "A" mode, see Fabian et al. 2001a for details). We tentatively assign the bands located at wavelengths larger than 20 μm to Ca–O vibrational modes.

The spectrum measured for the orientation of the field vector parallel to the c-axis is more complicated due to the presence of the interface layers in the crystal structure. An Al–O mode is also seen here at 12 μm, but additional bands show up in the 20 μm range, for which an assignment is not yet at hand.

From these spectra, two sets of optical constants have been derived by a Lorentz oscillator fit of the dielectric function (compare Fabian et al. 2001a) using 9 oscillators for each of the polarization directions. Figure 2 illustrates the wavelength dependence of the resulting complex indices of refraction. The optical constants have been made available for public access in the electronic database reachable via `http://www.astro.uni-jena.de` (see Henning et al. 1999).

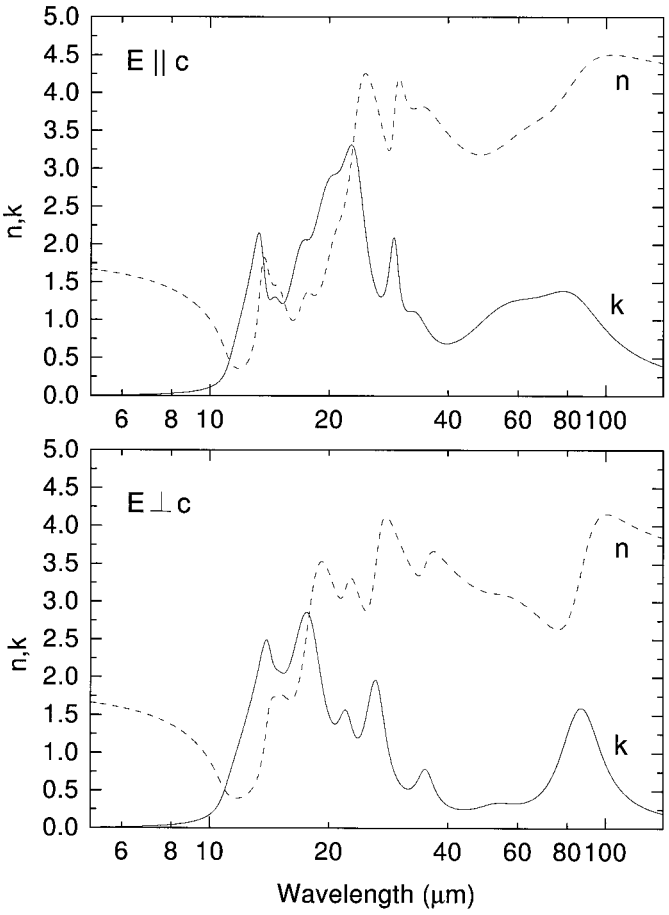

Fig. 2. Complex refractive index of hibonite single crystals in the IR for polarization parallel and perpendicular to the *c*-axis, respectively. The data have been calculated from the two solid curves in Fig. 1.

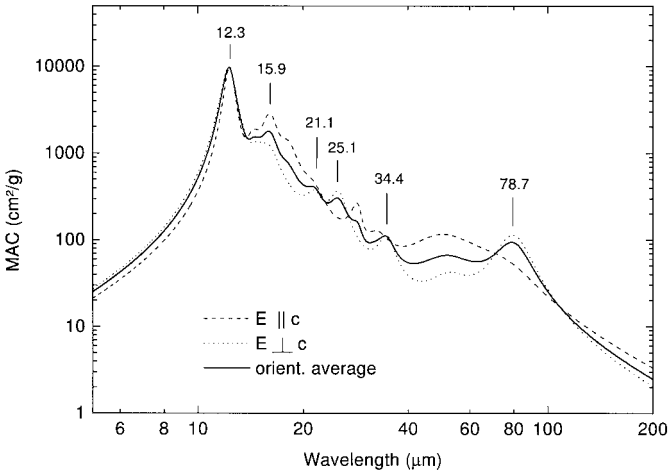

Fig. 3. Calculated mass absorption coefficient of spherical hibonite grains in the IR (solid line) and its decomposition into the contributions of the polarization directions parallel and perpendicular to the *c*-axis.

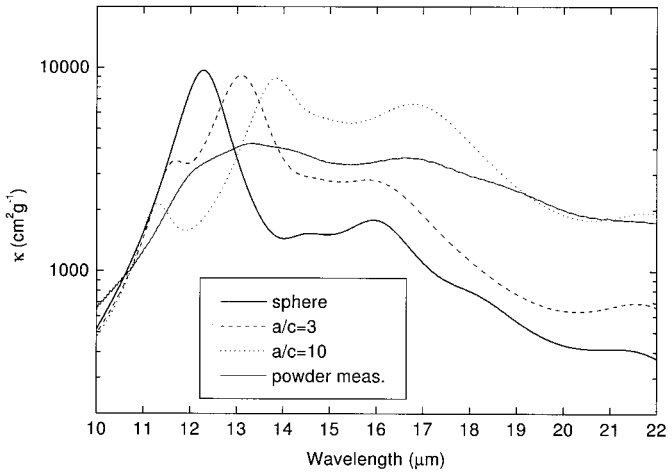

Fig. 4. The mass absorption coefficients of hibonite particles with different axis ratios (1:1, 1:3 and 1:10) compared to the mass absorption coefficient derived from a powder transmission spectrum.

3. The emissivity of small hibonite grains

The optical constants can be used to calculate the mass absorption coefficient (MAC) being representative of the emissivity of small hibonite grains in the infrared band region. Figure 3 shows the calculated MAC spectra for an ensemble of arbitrarily oriented single-crystal grains of spherical shape and the decomposition of this spectrum into the contributions of the orientations parallel and perpendicular to the *c*-axis. Both orientations together produce a main feature at about 12.3 μm, whereas the orientation parallel to the *c*-axis is responsible for a second major feature at about 15.9 μm. Further absorption bands occur at about 21.1, 25.1, 34.4, and 78.7 microns.

Whether a spherical grain shape, as assumed for the calculations above, does apply to the oxide condensates in a circumstellar atmosphere, however, is actually a matter of debate. The morphology of the meteoritic hibonite grains studied by Choi et al. (1999) is clearly plate-like. Furthermore, it is known from condensation experiments that crystalline oxide and silicate grains can be non-spherical (Rietmeijer et al. 2002; Tsuchyama 1998).

Nonsphericity of the grains would strongly affect the spectra. In Fig. 4 we present the calculated MAC in the 10–22 μm wavelength range for selected oblate ellipsoidal hibonite grains resembling the shapes of the plate-like meteoritic grains. As a consequence of this shape variation, the main feature produced by the hibonite grains is shifted by nearly 2 μm to 14 μm. The secondary feature is shifted towards 17 μm and is considerably enhanced in strength. An additional feature appears at a wavelength shorter than 12 μm.

It is evident that broad shape distributions summing up the features produced by different grain shapes would lead to a strong broadening of the emission bands. For spinel and other oxides, this fact has already been discussed by Posch et al. (1999). An illustration is given by the measured absorption spectrum of a powdered hibonite sample shown in Fig. 4 for comparison. It has to be noted, that in this case agglomeration of the grains embedded in a KBr matrix simulates a wide shape distribution with very elongated structures. The resulting very broad bands hardly could be identified in stellar spectra. Particles of such a wide shape distribution would contribute to

Table 1. Wavelength position λ_B, *FWHM* and maximum MAC of the main emission bands of spherical hibonite grains

λ_B [μm]	*FWHM* [μm]	MAC [cm^2 g^{-1}]
12.28	1.1	9700
15.93	2.2	1800
25.05	3.9	310
34.4	6.2	110
78.7	24.2	94

the background emissivity of oxygen-rich dust in the 11–17 μm wavelength range, i.e. in the trough between the two silicate bands. This is indeed found to be shallower than expected from the optical constants e.g. of amorphous olivine (see Dorschner 1999).

More moderate shape distributions would produce correspondingly narrower features with the central wavelength position depending on the mean shape. The presence of a relatively narrow 13 μm band and other features indicates that at least for part of the oxide dust population, the shape distribution is not very broad, if the identification with oxide grains is correct. The same statement seems to hold for the crystalline silicate grains in the outflows of evolved stars and in disk sources, where also some observed bands are narrower than those measured for grains embedded in KBr matrix (e.g. Molster et al. 2002; Fabian et al. 2001b).

The shape distribution of circumstellar hibonite grains, so far, is not known. Certainly, it is strongly dependent on the thermal and pressure conditions in these environments. We consider the probability non-negligible that a significant part of these grains is of spherical shape, although in contrast to spinel the crystal system does not seem to favourize spherical shapes. Condensation experiments are planned to address this question. In Table 1 we summarize the characteristics of the main bands for spherical grains.

4. Consequences for the identification of the hibonite bands in stellar spectra

If hibonite grains with a narrow shape distribution would be condensed in the outflows of oxygen-rich AGB stars with low mass-loss rates, we can conclude from our present experimental study that the wavelength position of their main infrared emission bands would strongly depend on the average shape. For near-spherical shapes, the main bands have to be expected at shorter wavelengths than those of (stoichiometric) spinel, namely at about 12.3 and 15.9 μm.

Unfortunately, in our search through ISO-SWS and LWS spectra, we could not find incontestable evidence for maxima of the observed flux at the predicted wavelengths, even though at 12.3 and 15.9 μm small humps seem to be present in some SWS spectra (e.g. of SW Vir and T Mic) and also in our mean profile. It is a problem, however, that the relative spectral response function (RSRF) of the ISO-SWS-01 band 3A, covering the wavelength range 12–16.5 μm, shows minima centered at 12.33 and 15.5 μm which may distort the observed feature shapes or might even generate pseudo-features (see Fig. 5). The apparent flux minimum near 12.3 μm does indeed seem to be artificial, since we find it to be present also in the SWS spectra of dust-free stars such as Vega or Arcturus. Considering the quite large width (*FWHM*) of the hibonite bands (see Table 1), the presence of these minima could actually lead to an artificial narrowing of the observed "features".

Concerning the relative strengths of the bands, it should be recalled that they are strongly dependent on the dust temperature. For the oxides considered here – if they are isolated from other grains – relatively low temperatures (see Posch et al. 2002) have to be expected in view of their transparency in the visual spectral range. This could lead to a strengthening of features at longer wavelengths compared to those at shorter ones.

The long-wavelength feature at 78.7 μm is quite strong and could serve as an actual proof of the presence of this mineral. However, by an examination of ISO-LWS spectra of R Dor, W Hya and R Hya, we could not find any broad emission band at the wavelength mentioned above. Note that there is a narrow emission line at 78.7 μm, prominent especially in the spectrum of W Hya, which is a H_2O line (see Barlow et al. 1996 for a detailed discussion).

This band would shift to a wavelength between 80 and 85 μm for elongated particle shapes whereas the weaker features in the 20–35 μm region are almost insensitive to shape effects. The main bands below 20 μm can shift strongly as shown in the previous section, which may even result in a contribution to the 12.95 and 16.8 μm "spinel features".

Since the maximum MAC of hibonite is almost as large as that of spinel, equal amounts of both dust species can be expected to produce emission features of comparable strength. It has already been shown by Kerschbaum et al. (2000) that if 2% of the total amount of dust of an oxygen-rich AGB star is composed of $MgAl_2O_4$, this is sufficient to account for the observed 13 μm emission feature provided that the dust temperature is homogeneous. For alternative carriers of this feature like α-Al_2O_3, similar results are found. Taking into account the cosmic abundance of Al, which is smaller than that of Mg and Si only by a factor of about 10, it follows that 20% of the available Al are needed to produce the 13 μm feature. Ca is about equally abundant as Al (solar system values). Therefore, if only 2% of the available Al and about 0.2% of the available Ca are locked in hibonite, this would be sufficient to produce a 12.3 μm feature consistent with the upper limits derived from the present observations.

These quite low numbers lead to the question where the residual aluminium may be hidden. One possible answer could be given in terms of an inhomogeneous dust temperature, which would reduce the emission by the cooler oxide grain population compared to iron-containing silicates (as mentioned above). Secondly, broad shape distributions could prevent oxide particles from producing bands which are sufficiently narrow to be detectable. A third possibility is that oxides may condense in an amorphous state – similarly to circumstellar silicates – which also leads to wide features (see Begemann et al. 1997). Our first experiments on condensation of aluminium oxide from a low-pressure gas environment indicate that this could indeed occur.

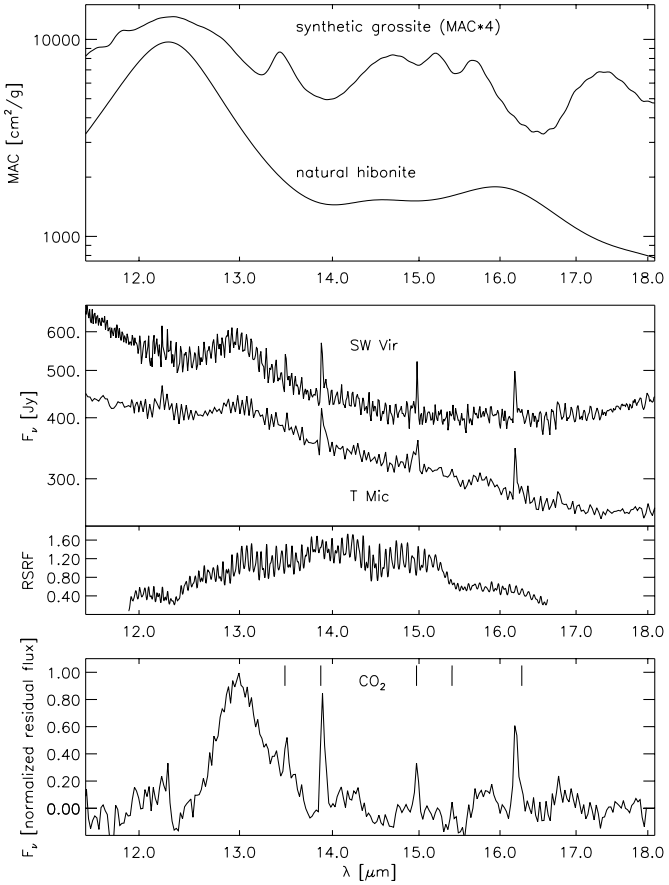

Fig. 5. *Upper panel*: The mass absorption coefficients of small spherical hibonite and grossite grains in the 12–18 μm region. For clarity, the MAC of grossite has been multiplied by a factor of 4. *Middle panels*: The ISO spectra of T Mic (SWS01) and SW Vir (SWS06, scaled as indicated) confronted with the response function for SWS band 3A. At 12.3 and 15.5 μm, the RSRF has prominent minima which are likely to distort the observed spectra (see text). *Lower panel*: Average residual emission profile derived from 23 ISO spectra by Fabian et al. (2001).

In view of the formation processes of Ca-Al oxides mentioned in Sect. 1, it is logical also to consider the more calcium-rich mineral grossite ($CaAl_4O_7$) as a potential circumstellar condensate. Indeed this mineral is one of the major components of CAIs. Because of the lack of larger natural crystals, we have synthesized a polycrystalline grossite sample from $CaCO_3$ and Al_2O_3 in an electric-arc furnace. The absorption spectrum of the powdered material embedded in KBr is shown at the top of Fig. 5. The main absorption feature is located at 12.3 μm just as in the case of hibonite, indicating the presence of tetrahedrally coordinated aluminium. A number of other bands is also seen in the wavelength range 13–18 μm and beyond. The more complex spectrum compared to hibonite is due to the monoclinic lattice structure of grossite (see Weber & Bischoff 1994).

Note that the shape of the grains, their agglomeration in the KBr environment and the polarization effect of the KBr matrix may influence the band positions and profiles in this spectrum. Therefore, an effort to identify grossite bands in ISO spectra seems to be too tentative as well. The uppermost curve in Fig. 5 is only meant to give an idea which features can serve as a key for the identification of circumstellar $CaAl_4O_7$.

We suggest to make further observations in order to clarify the presence and strength especially of the predicted 12.3, 15.9, ~25, ~35 and ~79 μm features. As far as the first one is concerned, ground-based observations should be sufficient for a detection, if a resolution of about 400 and a S/N-ratio near 100 is achieved. For the remaining features, space-borne observatories will be necessary.

5. Conclusion and outlook

If our recent assignment of the 13, 16.8 and 32 μm emission bands to spinel is correct, then – considering the cosmic element abundance and recent results in meteoritics – calcium aluminium oxides like hibonite and grossite are likely to form in the envelopes of oxygen-rich AGB stars. In this paper we have measured optical constants and transmission spectra, respectively, of these minerals in order to provide basic data necessary for the identification of infrared emission bands produced by hibonite and grossite grains.

In view of problems with the ISO-SWS response function at the wavelengths 12.3 and 15.5 μm, further observations are needed for such an identification and to examine their relation to the spinel dust emission features. Ground-based observations as well as the spectra obtainable with the Space Infrared Telescope Facility (SIRTF) and ESA's Far Infrared and Submillimeter Telescope Herschel (HSO) will contribute to understanding the formation of circumstellar oxides.

Acknowledgements. This work was supported by grant number Mu 1164/5–1 of the *Deutsche Forschungsgemeinschaft, DFG*. We thank Gabriele Born and Walter Teuschel for helping with the preparative work and the measurements as well as Dr. Vera Hammer (Naturhistorisches Museum Wien) for providing us with hibonite samples. Further we are grateful to Dr. Frank J. Molster (ESTEC) for very useful comments on the manuscript and support with the interpretation of ISO spectra. TP received a DOC grant [Doktorandenprogramm der Österreichischen Akademie der Wissenschaften] and travel grants from the project FIRST-PACS/Phase I, financed by the Austrian Federal Ministry of Transport, Innovation and Technology (bm:vit).

References

Barlow, M. J., Nguyen-Q-Rieu, Truong-Bach, et al. 1996, A&A, 315, L241
Beevers, C. A., & Ross, M. A. S. 1937, Z. Krist., 97, 59
Begemann, B., Dorschner, J., Henning, Th., et al. 1997, ApJ, 476, 199
Bragg, W. L., Gottfried, C., & West, J. 1931, Z. Krist., 77, 255
Brearley, A. J., & Jones, R. H. 1998, in Rev. in Mineralogy, ed. J. J. Papike, 36, 3
Choi, B.-G., Wasserburg, G. J., & Huss, G. R. 1999, ApJ, 522, L133
Curien, H., Guillemin, C., Orcel, J., & Sternberg, M. 1956, Compt. Rend., 242, 2845
Dorschner, J. 1999, in Formation and Evolution of Solids in Space, ed. J. M. Greenberg, & A. Li (Dordrecht: Kluwer), 229
Fabian, D., Posch, Th., Mutschke, H., et al. 2001a, A&A, 373, 1125
Fabian, D., Henning, Th., Jäger, C., et al. 2001b, A&A, 378, 228
Fahey, A. J., Zinner, E., Kurat, G., & Kracher, A. 1994, Geochim. Cosmochim. Acta, 58, 4779

Fegley, M. B. 1992, Lunar Planet. Sci., 13, 211
Henning, T., Il'in V. B., Krivova, N. A., et al. 1999, A&AS, 136, 405
Hron, J., Aringer, B., & Kerschbaum, F. 1997, A&A, 322, 280
Justtanont, K., Feuchtgruber, H., de Jong, T., et al. 1998, A&A, 330, L 17
Kato, K., & Saalfeld, H. 1968, N. Jb. Miner. Abh., 109, 192
Kerschbaum, F., Posch, Th., & Aringer, B. 2000, in Proc. Conf., ISO beyond the Peaks, Villafranca del Castillo, Spain (ESA SP-456)
Krot, A. N., Huss, G. R., & Hutcheon, I. D. 2001, Meteoritics Planet. Sci. Suppl., 36, A105.
Kurat, G. 1975, Tschermaks Min. Petr. Mitt., 22, 38
Molster, F. J., Waters, L. B. F. M., & Tielens, A. G. G. M. 2002, A&A, 382, 222
Posch, Th., Kerschbaum, F., Mutschke, H., et al. 1999, A&A, 352, 609
Posch, Th., Mutschke, H., & Fabian, D. 2002, Hvar Obs. Bull., submitted
Sloan, G. C., LeVan, P. D., & Little-Marenin, I. R. 1996, ApJ, 463, 310
Rietmeijer, F. J. M., Hallenbeck, S. L., Nuth, J. A., & Karner, J. M. 2002, Icarus, 156, 269
Speck, A. K., Barlow, M. J., Sylvester, R. J., & Hofmeister, A. M. 2000, A&AS, 146, 437
Tsuchiyama, A. 1998, Mineral. J., 20, 59
Ulyanov, A. A. 1998, in Advanced Mineralogy, vol. 3, ed. A. S. Marfunin (Springer-Verlag, Berlin), 47
Weber, D., & Bischoff, A. 1994, Eur. J. Miner., 6, 591